

Supplementary Materials for **Monitoring reservoir response to earthquakes and fluid extraction, Salton Sea geothermal field, California**

Taka'aki Taira, Avinash Nayak, Florent Brenguier, Michael Manga

Published 10 January 2018, *Sci. Adv.* **4**, e1701536 (2018)

DOI: 10.1126/sciadv.1701536

This PDF file includes:

- fig. S1. Map view of the seismicity at the SSGF.
- fig. S2. Time delay measurements obtained from EN network at the SSGF.
- fig. S3. Frequency-dependent Rayleigh-wave phase velocity sensitivity.
- fig. S4. Time-lapse measurements of seismic velocity changes inferred from nine components of NCFs.
- fig. S5. Stress changes imparted by the 4 April 2010 M_w 7.2 El Mayor–Cucapah earthquake.
- fig. S6. Stress changes imparted by the 26 August 2012 M_w 5.4 Brawley earthquake.
- fig. S7. Seismic velocity changes, geodetic line-length change, and precipitation measurements around occurrence times of the 2010 M_w 7.2 El Mayor–Cucapah earthquake and the 2012 Brawley seismic (BS) swarm.
- fig. S8. Seismic velocity changes, net production, and geodetic line-length change measurements.
- fig. S9. Time history of velocity changes with the single-station cross-correlation analysis.
- fig. S10. Long-term velocity change estimate with curve fitting.
- fig. S11. Long-term velocity change as a function of site elevation.
- fig. S12. Time-lapse measurements of seismic velocity changes at station RXH with the single-station cross-correlation analysis.
- fig. S13. Response of hydrothermal vents to stresses.
- fig. S14. Stress sensitivity for the 2010 M_w 7.2 El Mayor–Cucapah earthquake.
- fig. S15. Seismic velocity changes, geodetic line-length change, and precipitation measurements around occurrence times of the 30 December 2009 M 5.8 Delta,

Baja California, Mexico and the 15 June 2010 M 5.7 Ocotillo, California earthquakes.

- fig. S16. Seismic velocity changes, geodetic line-length change, and precipitation measurements around occurrence times of the 2009 and 2010 earthquake swarms.
- fig. S17. Volumetric static stress change and seismicity map.
- fig. S18. Possible velocity change during the 2005 OB earthquake swarm.
- fig. S19. The November 2009 earthquake swarm.
- fig. S20. The December 2010 earthquake swarm.
- table S1. Parameters of the best-fitting curve to observed seismic velocity changes with Eq. 1 and variance reduction (VR).
- table S2. PGV from the SCEDC and stress sensitivity estimate for the 4 April 2010 M_w 7.2 El Mayor–Cucapah earthquake.
- References (78–80)

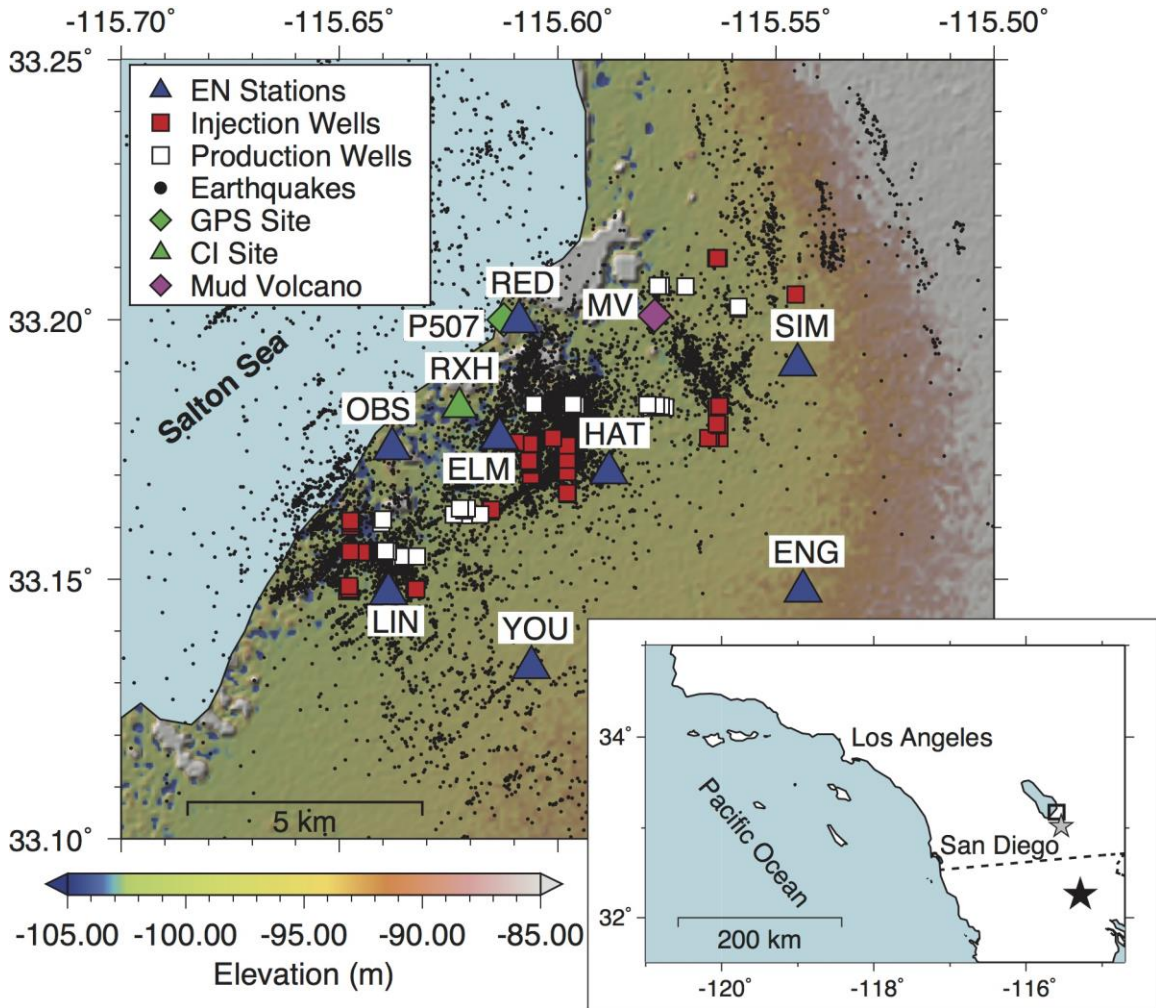


fig. S1. Map view of the seismicity at the SSGF. The blue triangles are the locations of the CalEnergy seismic network (EN network). Also shown are the locations of the geothermal injection (red squares) and production wells (white squares) obtained from the California Department of Conservation. Green triangle and diamond are the locations of seismic station RXH and continuous Global Positioning System (GPS) site P507, respectively. Black dots are the relocated earthquake locations (1981-2016) (77). Purple diamond is the location of Davis-Schrimpf mud volcanoes. Inset map shows the location of the SSGF (black rectangle) in southern California and the northern part of Baja California. Also shown are the epicenters of the 4 April 2010 M_w 7.2 El Mayor-Cucapah

earthquake (solid star) and the 26 August 2012 M_w 5.4 Brawley earthquake (gray star).

The dashed line shows the border between United States and Mexico.

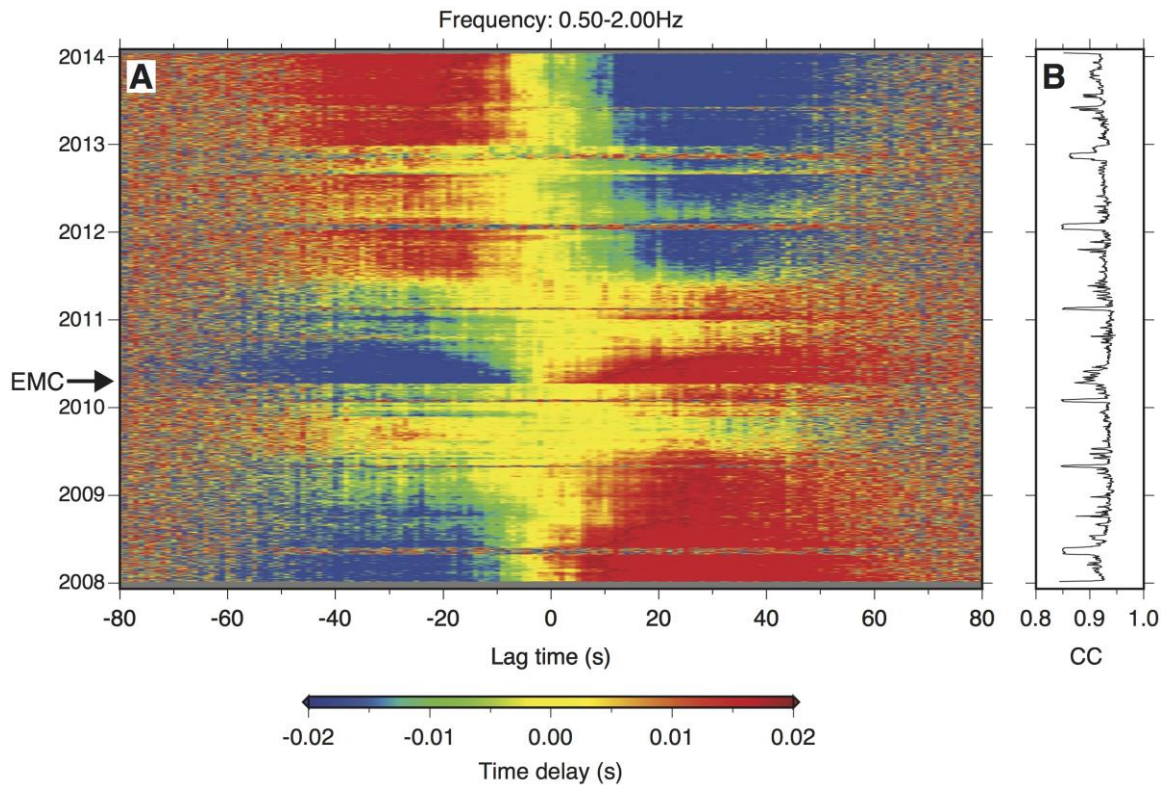


fig. S2. Time delay measurements obtained from EN network at the SSGF. (A)

Time delay (dt) measurement in a frequency range of 0.5-2.0 Hz between the reference and the 5-day stack of noise cross-correlation functions (NCFs) as a function of lag time. Average dt values over all possible pairs are plotted by the color code in the bottom of this figure. **(B)** Cross-correlation (CC) averaged over all pairs of stations. There are a number of time periods in which the CC suddenly decreased, and consequently the time delay measurements are unstable during those time periods. Time periods in which we were not able to recover empirical Green's functions are marked by gray areas in Fig. 1.

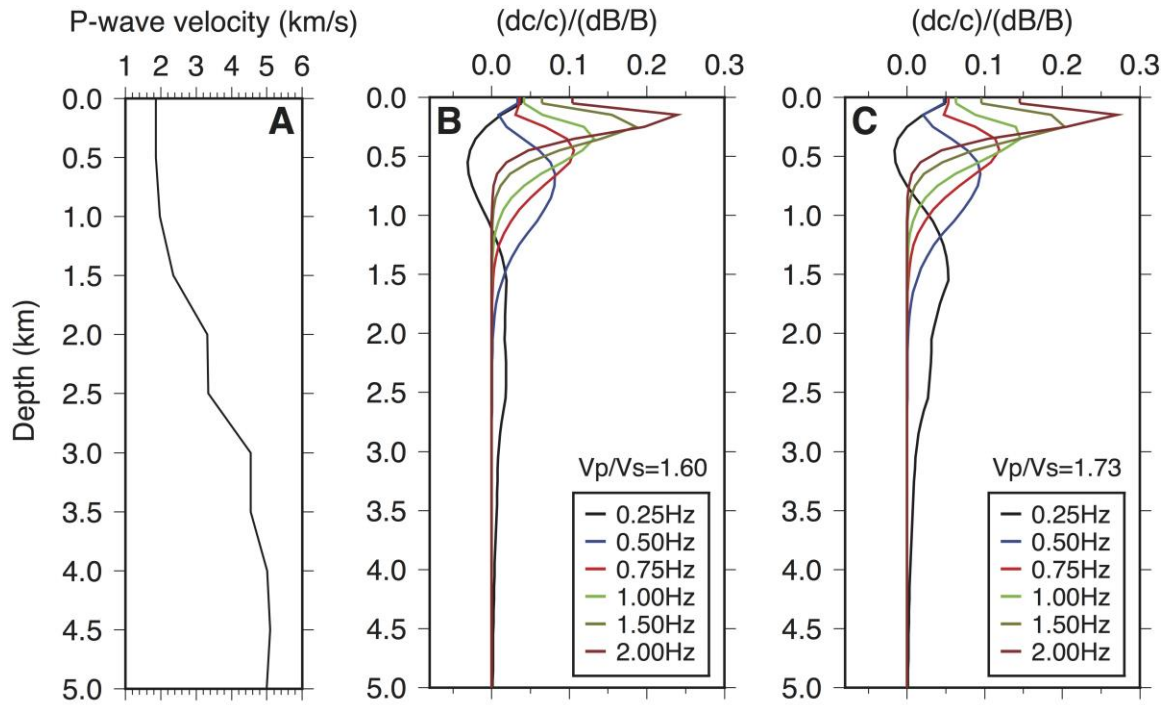


fig. S3. Frequency-dependent Rayleigh-wave phase velocity sensitivity. (A) A one-dimensional (1D) P -wave velocity (V_p) model (66) to derive the 1D S -wave velocity (V_s) model for surface-wave sensitivity kernel estimate. Rayleigh-wave sensitivity kernels assuming with (B) $V_p/V_s = 1.60$ (67) and (C) $V_p/V_s = 1.73$ (78). Computer Programs in Seismology package (79) was used for estimating the sensitivity kernels. Two sets of the sensitivity kernels with different V_p/V_s are comparable.

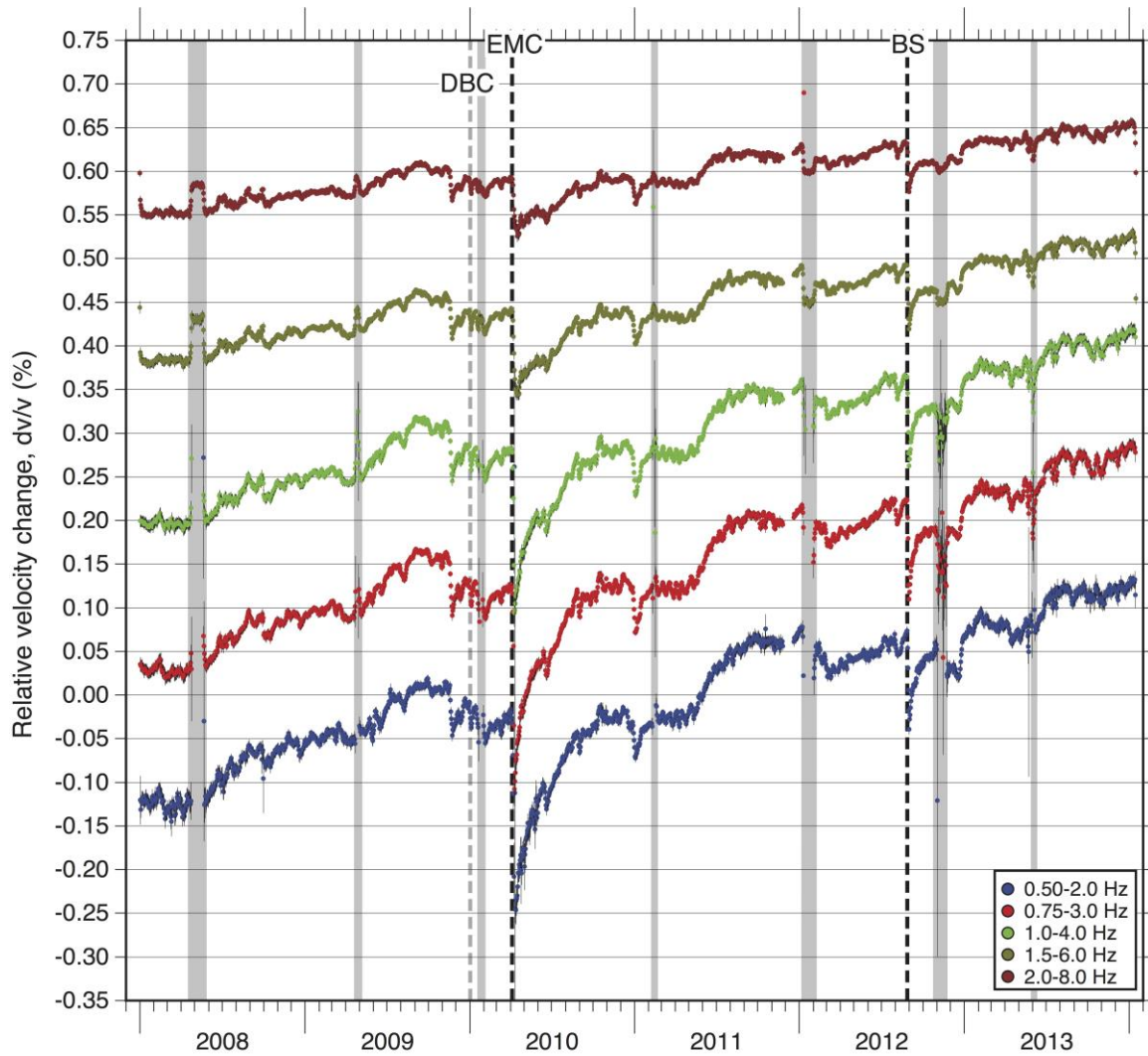


fig. S4. Time-lapse measurements of seismic velocity changes inferred from nine components of NCFs. Time history of seismic velocity (dv/v) by averaging 9 components of noise cross-correlation functions with two sigma standard deviations at five different frequency bands during December 2007 through January 2014. EMC, BS, and DBC represent the 2010 M_w 7.2 El Mayor-Cucapah earthquake, the 2012 Brawley Seismic swarm, the 30 December 2009 M 5.8 Delta, Baja California, Mexico, respectively (vertical dashed lines). Gray areas indicate time windows in which we were not able to recover empirical Green's functions (fig. S2 and Materials and Methods).

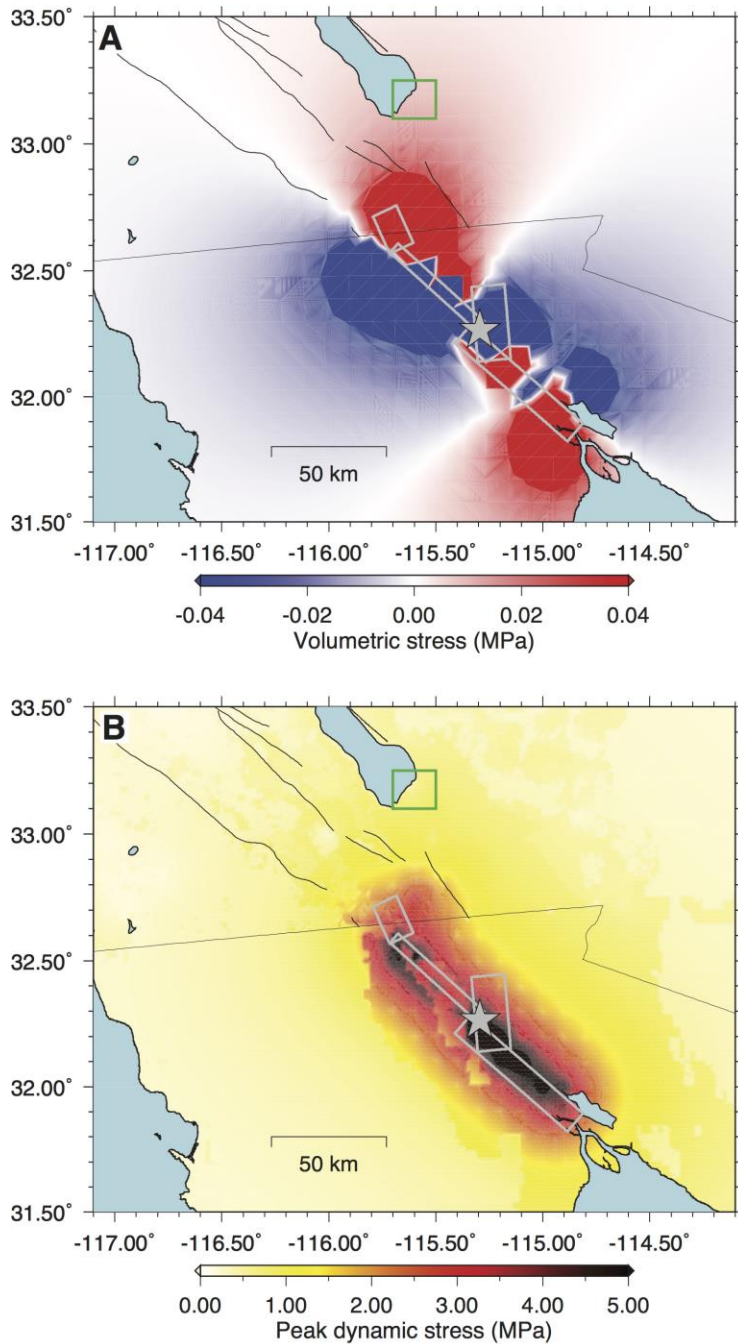


fig. S5. Stress changes imparted by the 4 April 2010 M_w 7.2 El Mayor–Cucapah earthquake. (A) Volumetric static stress change at a depth of 1 km. (B) Peak dynamic stress change. Gray star is the hypocenter of the 2010 M_w 7.2 El Mayor-Cucapah earthquake, and gray rectangles are the fault planes obtained from (64). Green rectangle is the SSGF region shown in fig. S1.

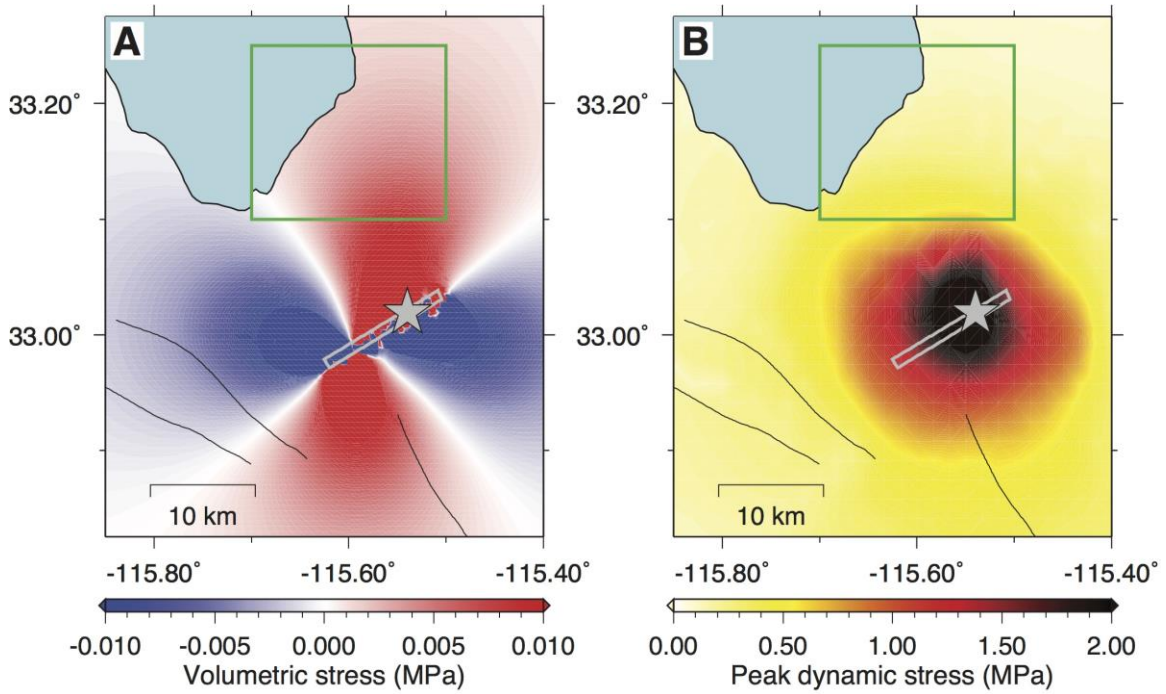


fig. S6. Stress changes imparted by the 26 August 2012 M_w 5.4 Brawley earthquake.

(A) Volumetric static stress change at a depth of 1 km. (B) Peak dynamic stress change.

Gray star is the hypocenter of the 2012 M_w 5.4 Brawley earthquake, and gray rectangle is the fault plane obtained from (65). Green rectangle is the SSGF region shown in fig. S1.

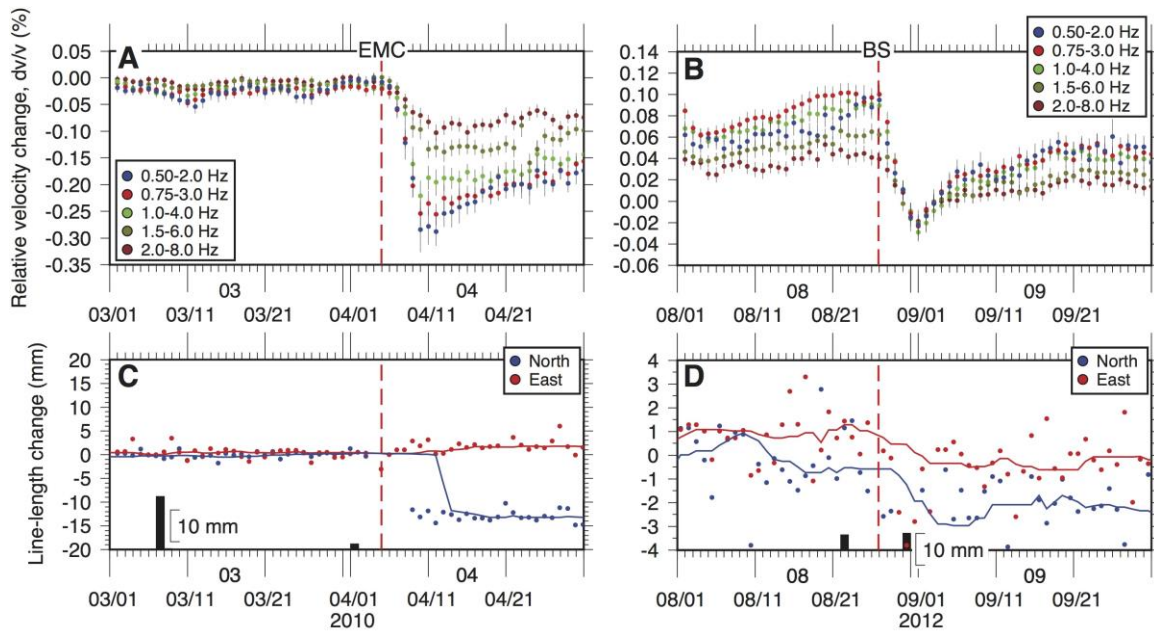


fig. S7. Seismic velocity changes, geodetic line-length change, and precipitation measurements around occurrence times of the 2010 M_w 7.2 El Mayor–Cucapah earthquake and the 2012 Brawley seismic (BS) swarm. (A and B) Time history of seismic velocity (dv/v) with five different frequency bands in the time intervals March–April 2010 and August–September 2012. (C and D) Horizontal Global Positioning System (GPS) line-length change between stations P507 and P505. GPS solutions (detrended data) determined by U.S. Geological Survey (<https://earthquake.usgs.gov/monitoring/gps>) were used. The location of station P507 is shown in fig. S1 and station P505 is located about 30 km north of station P507. Blue and red lines are a 10-days median GPS data in north-south and east-west components, respectively. Permanent static offsets of ~ 1.5 cm and ~ 2.0 mm were observed in the North-South line-length change (blue circles) following the EMC earthquake and the BS swarm, respectively. It should be noted however that the one-sigma error ranges from 2-5 mm for both horizontal components. Also shown is the daily precipitation (black bars) collected at Fish Creek Mountains (station code FIS, ~ 45 km east from the SSGF)

extracted from the California Department of Water Resources, Data Exchange Center
(<http://cdec.water.ca.gov>).

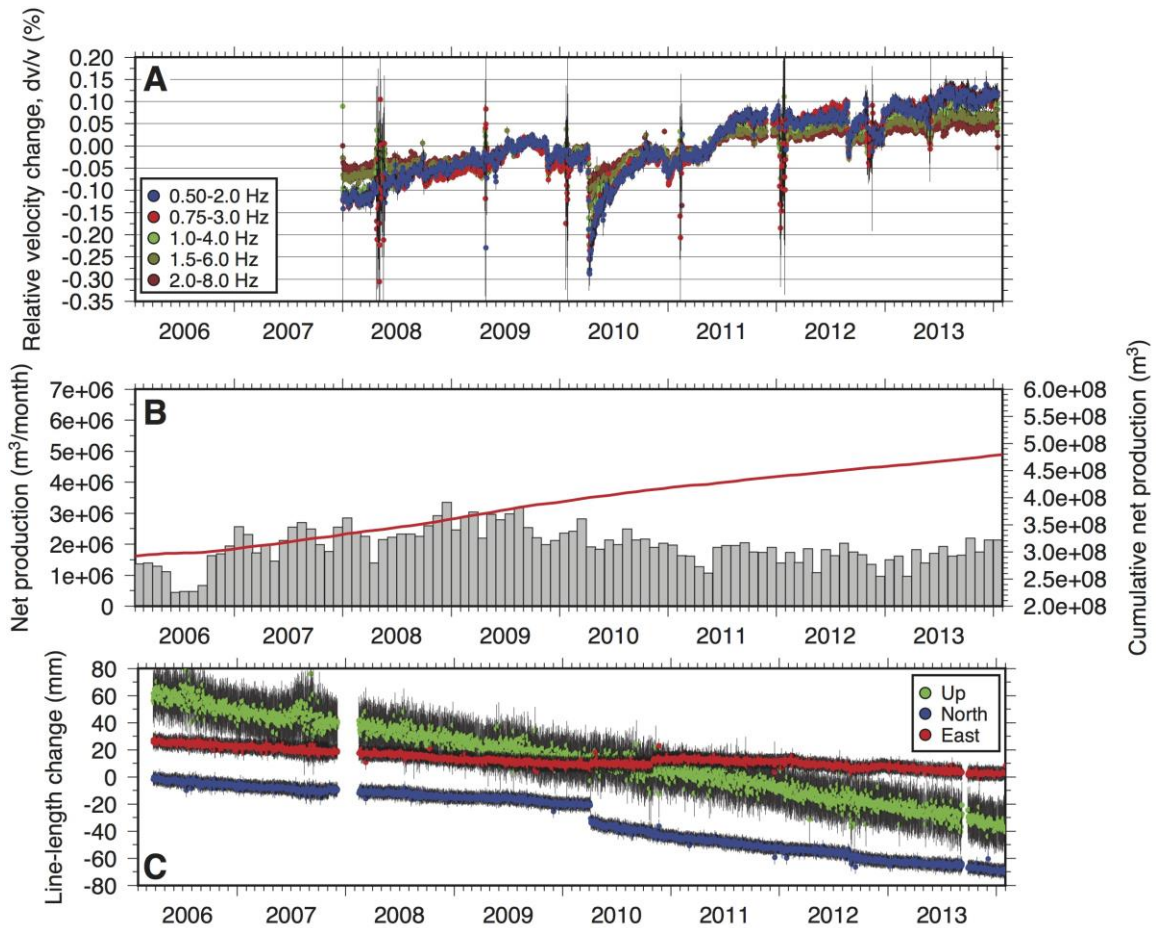


fig. S8. Seismic velocity changes, net production, and geodetic line-length change measurements. (A) Time history of seismic velocity (dv/v) with five different frequency bands in the time interval December 2007 through January 2014. (B) Gray bars represent the monthly net production at the SSGF starting from February 2006 (4). Also shown is the cumulative net production (red line). (C) Global Positioning System (GPS) line-length change between stations P507 and P505 with the one-sigma error bars. The location of station P507 is shown in fig. S1 and station P505 is located about 30 km north of station P507. We used GPS solution determined by U.S. Geological Survey (<https://earthquake.usgs.gov/monitoring/gps>). Both GPS sites have been operational since 2005-2006 to provide continuous GPS data.

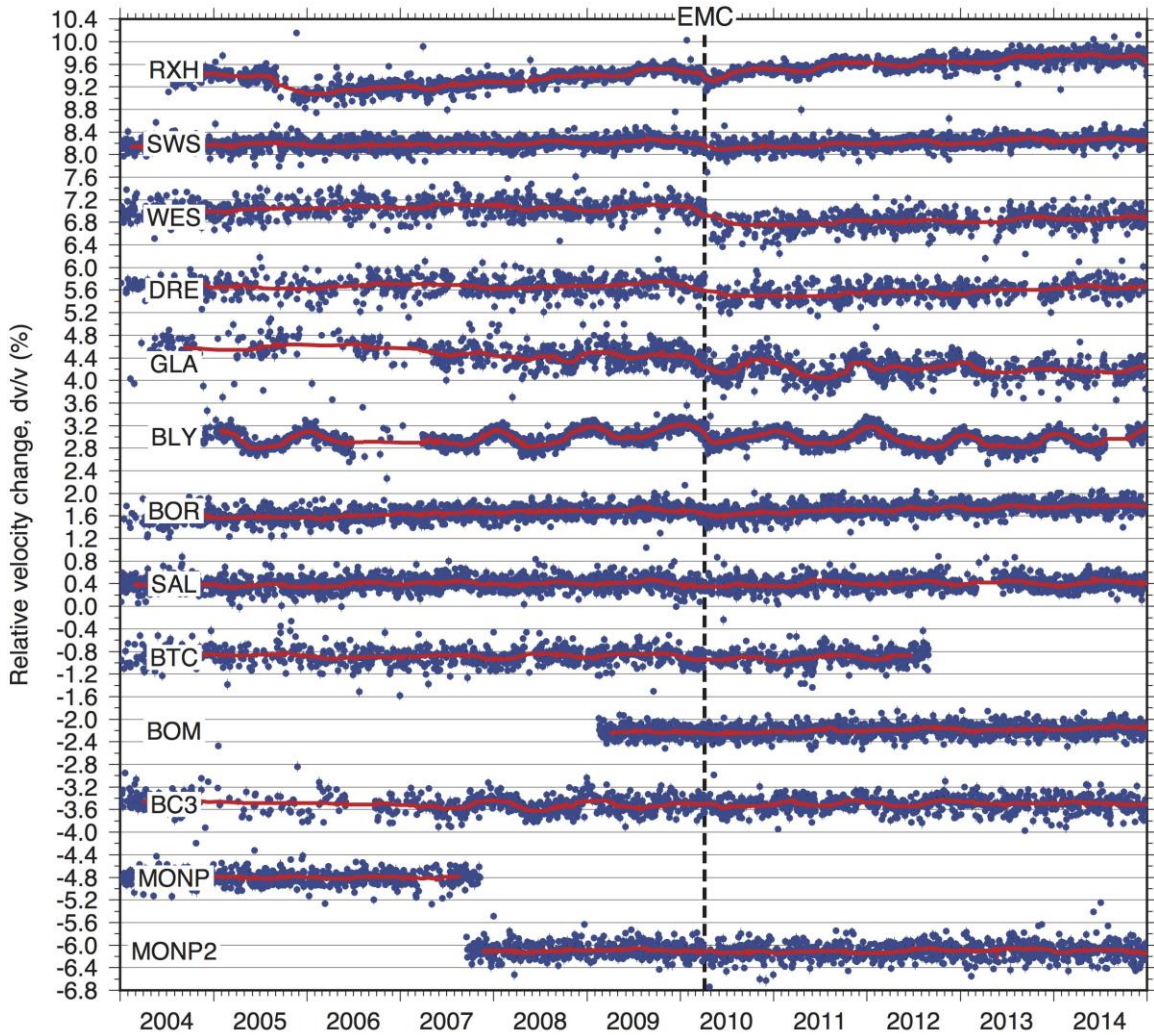


fig. S9. Time history of velocity changes with the single-station cross-correlation analysis. Blue dots are the velocity changes in a frequency range of 0.5-2.0 Hz. Red lines are velocity change measurements with the 60-day running median filter. Velocity change measurements with uncertainty (two-sigma standard deviations) less than 0.1% were plotted. Black dashed line is the occurrence time of the 2010 M_w 7.2 El-Mayor Cucapah (EMC) earthquake.

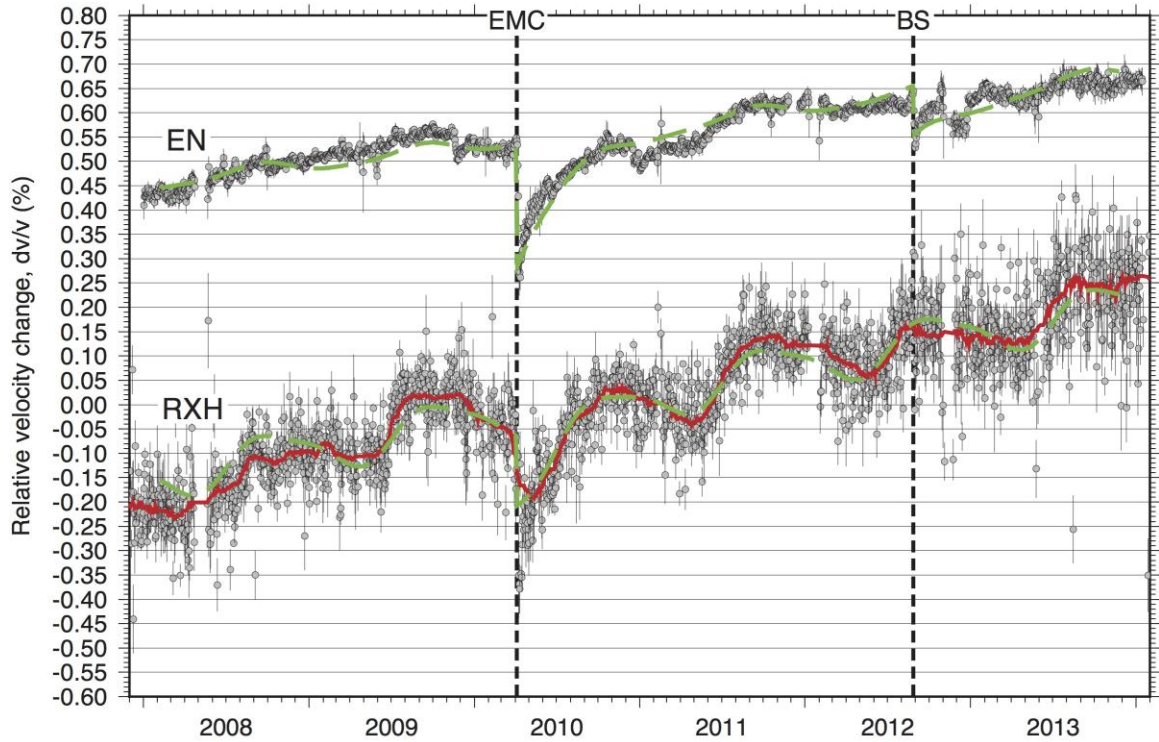


fig. S10. Long-term velocity change estimate with curve fitting. Gray dots are the velocity changes in a frequency range of 0.5-2.0 Hz. Red line represents velocity change measurements with the 60-day running median filter for the single-station cross-correlation analysis of station RXH. EN represents the two-station cross-correlation analysis of the CalEnergy stations. Green dashed lines are the best-fitting curves with equation (1). EMC and BS represent the 2010 M_w 7.2 El Mayor-Cucapah earthquake and the 2012 Brawley Seismic swarm, respectively.

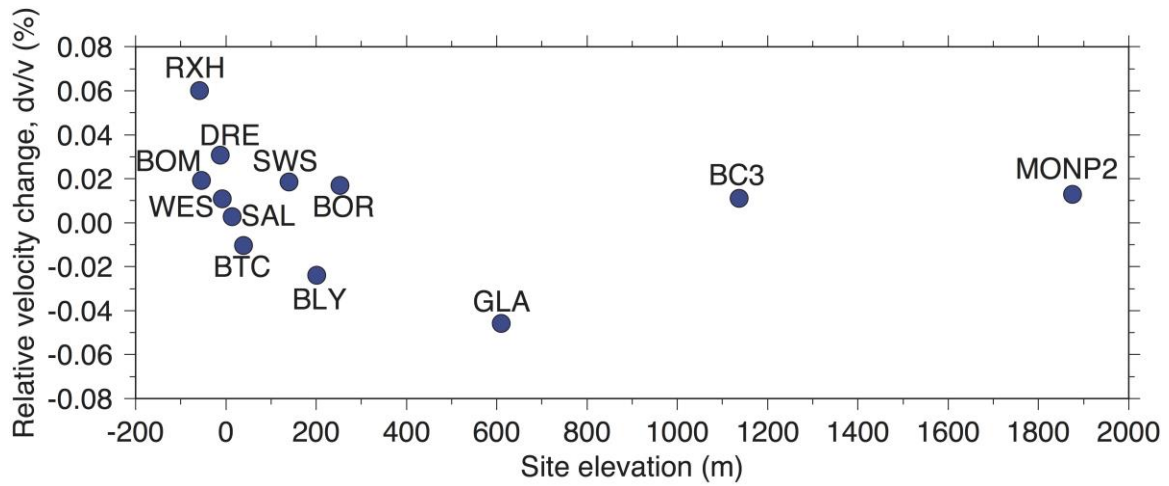


fig. S11. Long-term velocity change as a function of site elevation. Blue dots are long-term velocity changes (dv/v) in a frequency range of 0.5-2.0 Hz.

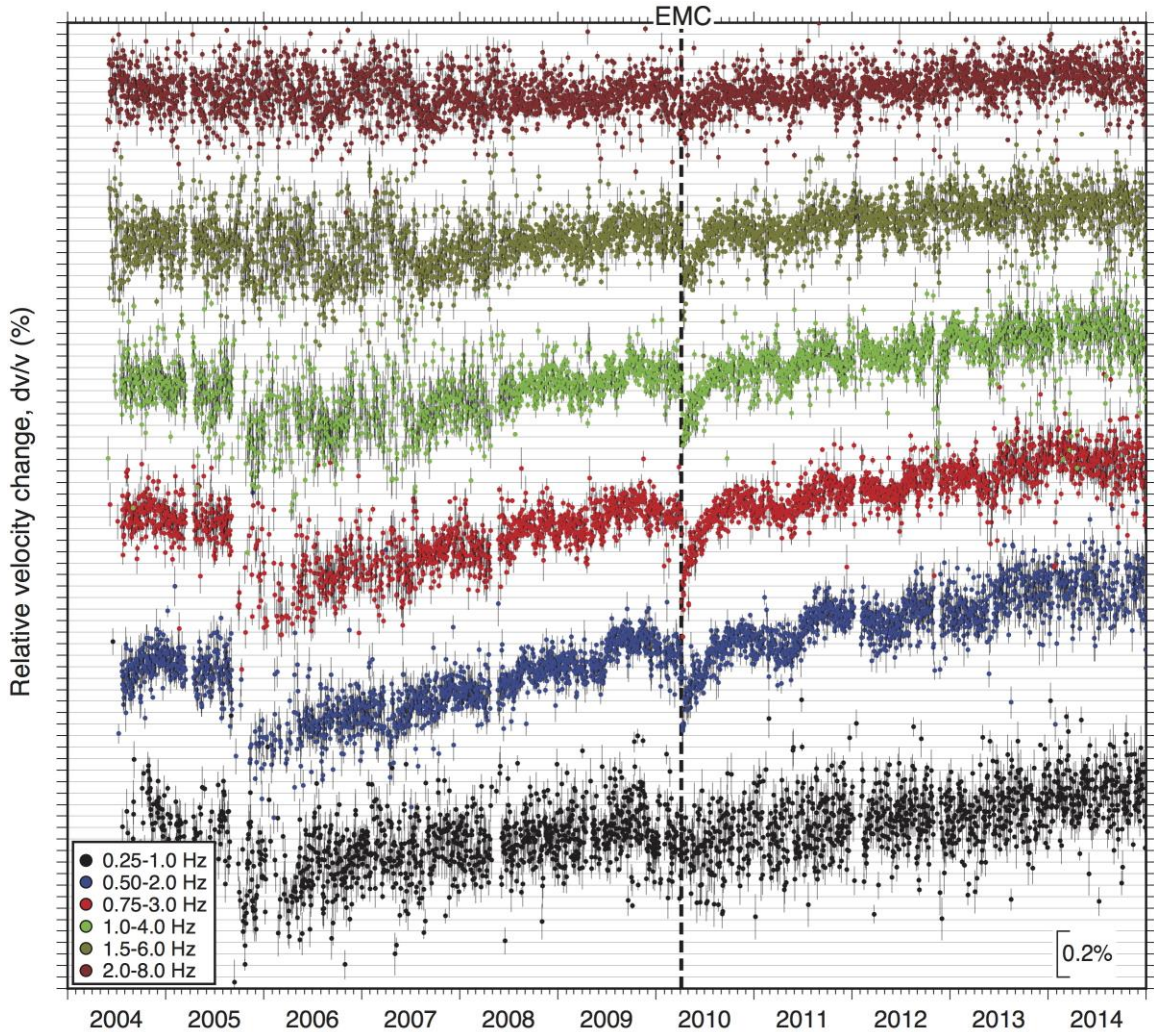


fig. S12. Time-lapse measurements of seismic velocity changes at station RXH with the single-station cross-correlation analysis. Time history of seismic velocity (dv/v) with two sigma standard deviations at six different frequency bands. Red lines are velocity change measurements with the 60-day running median filter. Velocity change measurements with uncertainty (two-sigma standard deviations) less than 0.1% were plotted. Black dashed line is the occurrence time of the 2010 M_w 7.2 El-Mayor Cucapah (EMC) earthquake.

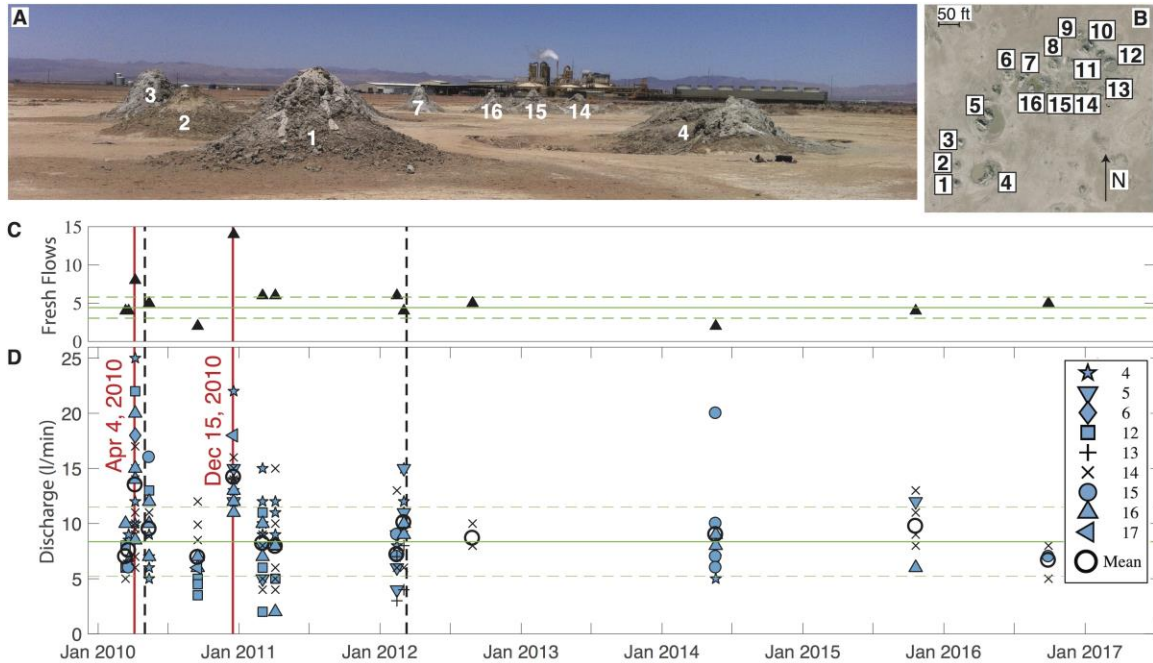


fig. S13. Response of hydrothermal vents to stresses. (A) Photo of the Davis-Schrimpf mud volcanoes with the 49 MW Hudson Ranch I geothermal plant in the background (photo 19 May, 2014). (B) Air photo of the vents showing the numbering scheme (numbers added to the visible mud volcanoes in (A)). (C) Total number of fresh flows and (D) gas discharge collected during campaign measurements. The first 4 sets of measurements were reported in (80), the next 6 are documented in (34) and the final 4 sets of measurements are previously unpublished. Each symbol corresponds to a specific vent whose location is shown in B. Spattered mud from the vents creates cones that can limit direct access to the mud and hence can prevent gas discharge from being measured. As a consequence, the number of measurements on a given day is variable. A clear increase in activity followed the 2010 El Mayor-Cucapah earthquake (80) and a magnitude 4.4 earthquake 19 km away from the vents on 15 December 2010 (34). The horizontal green lines show mean values with the standard deviation being indicated with the horizontal dashed green lines. The bold open circle is the mean gas discharge. The times of the two earthquakes that preceded the increases in discharge and number of fresh flows are shown with the vertical red lines. The vertical black lines indicate the date on which the adjacent Hudson Ranch geothermal facility was first commissioned and then

when production began. There is no obvious effect of the geothermal plant on these hydrothermal vents.

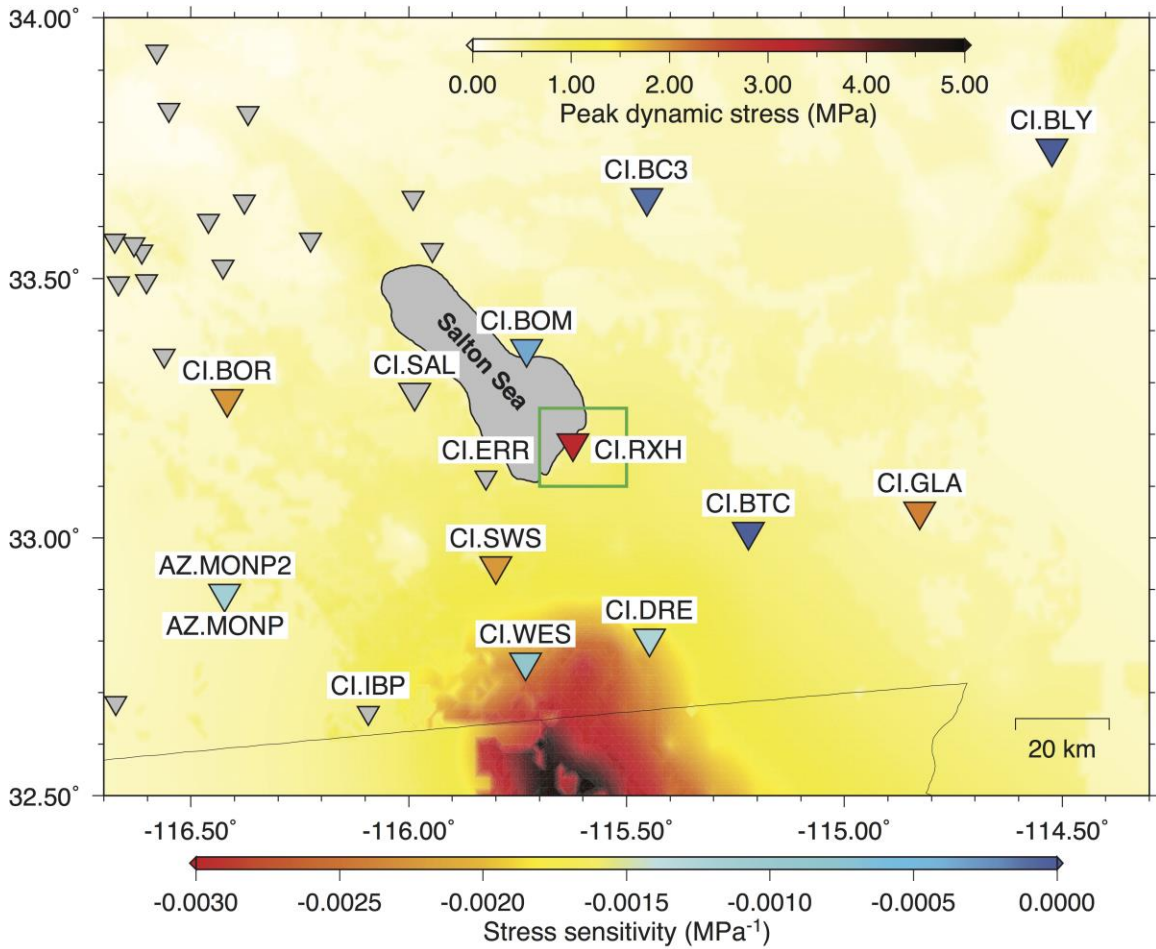


fig. S14. Stress sensitivity for the 2010 M_w 7.2 El Mayor–Cucapah earthquake.

Values of the stress sensitivity in a frequency range of 0.5-2.0 Hz obtained from curve fitting (table S2 and Materials and Methods) are shown by the color code in the bottom of the figure. Background color represents the peak dynamic stress inferred from the peak ground velocity measurements obtained from the Southern California Earthquake Data Center (Materials and Methods). Green rectangle is the SSGF region shown in fig. S1.

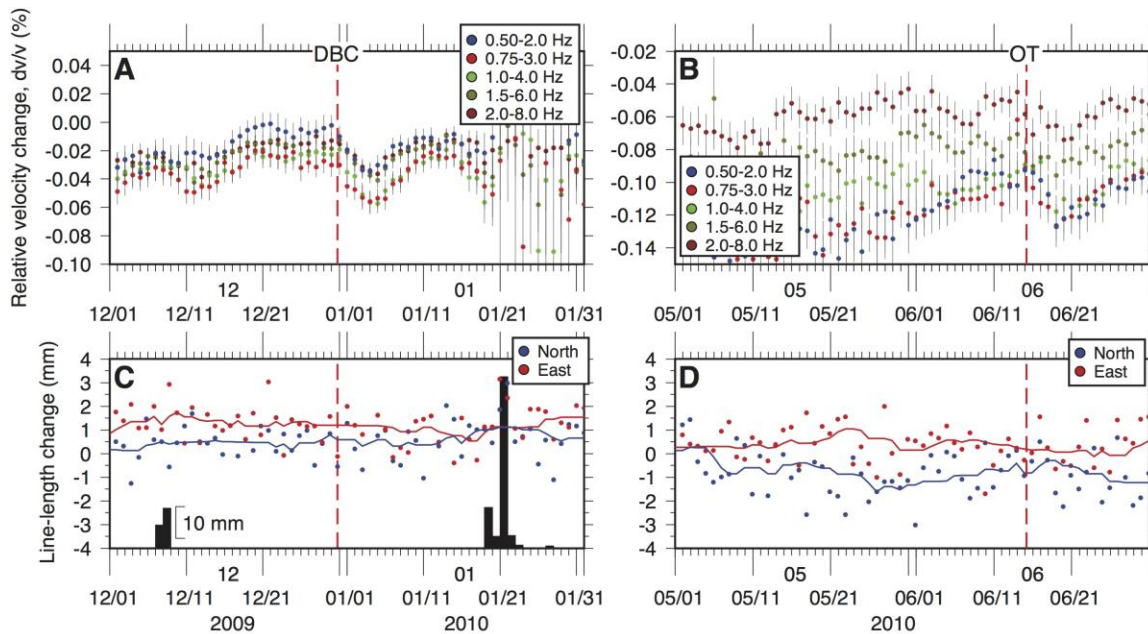


fig. S15. Seismic velocity changes, geodetic line-length change, and precipitation measurements around occurrence times of the 30 December 2009 M 5.8 Delta, Baja California, Mexico and the 15 June 2010 M 5.7 Ocotillo, California earthquakes. (A and B) Time history of seismic velocity (dv/v) with five different frequency bands in the time intervals March-April 2010 and August-September 2012. Note that the OT earthquake occurred about 2 months after the 2010 M_w 7.2 El-Mayor Cucapah (EMC) earthquake, and the large variations in velocity change before the OT earthquake are related to the EMC post-seismic recovery process. (C and D) Horizontal Global Positioning System (GPS) line-length change between stations P507 and P505. GPS solutions (detrended data) determined by U.S. Geological Survey (<https://earthquake.usgs.gov/monitoring/gps>) were used. The one-sigma error ranges from 2-5 mm for both horizontal components. The location of station P507 is shown in fig. S1 and station P505 is located about 30 km north of station P507. Blue and red lines are a 10-days median GPS data in north-south and east-west components, respectively. Also shown is the daily precipitation (black bars) collected at Fish Creek Mountains (station

code FIS, ~45 km east from the SSGF) extracted from the California Department of Water Resources, Data Exchange Center (<http://cdec.water.ca.gov>).

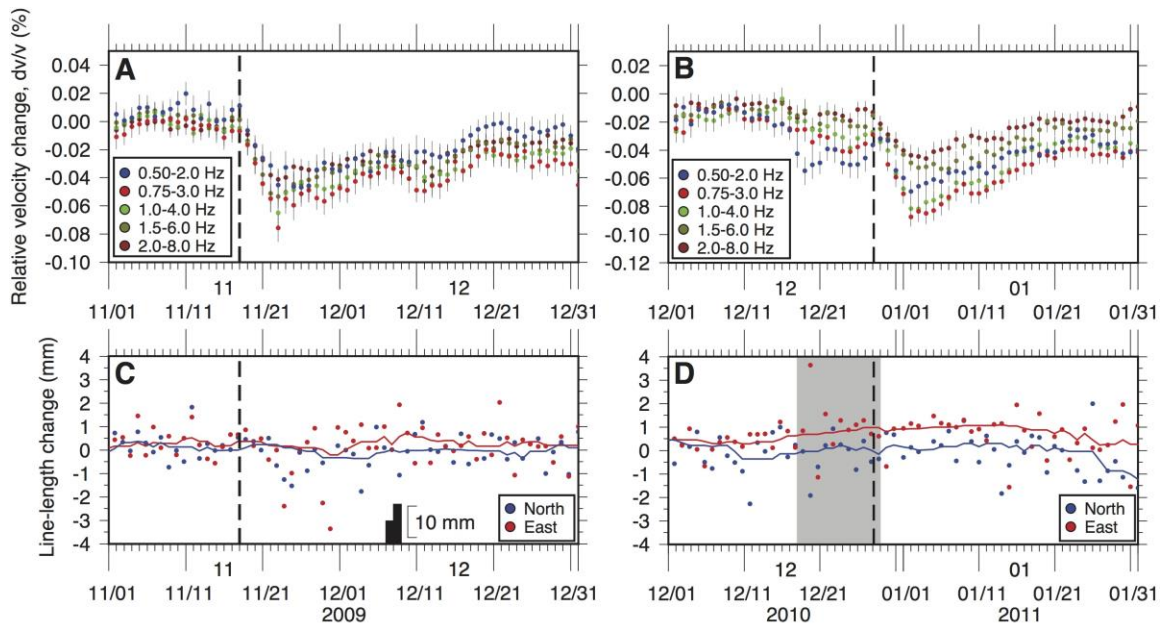


fig. S16. Seismic velocity changes, geodetic line-length change, and precipitation measurements around occurrence times of the 2009 and 2010 earthquake swarms.

(A and B) Time history of seismic velocity (dv/v) with five different frequency bands in the time intervals March-April 2010 and August-September 2012. (C and D) Horizontal Global Positioning System (GPS) line-length change between stations P507 and P505.

GPS solutions (detrended data) determined by U.S. Geological Survey

(<https://earthquake.usgs.gov/monitoring/gps>) were used. The one-sigma error ranges from 2-5 mm for both horizontal components. The location of station P507 is shown in fig. S1 and station P505 is located about 30 km north of station P507. Blue and red lines are a 10-days median GPS data in north-south and east-west components, respectively. Also shown is the daily precipitation (black bars) collected at Fish Creek Mountains (station code FIS, ~45 km east from the SSGF) extracted from the California Department of Water Resources, Data Exchange Center (<http://cdec.water.ca.gov>). Gray-filled area in (D) indicates that the precipitation data were not available during this time period.

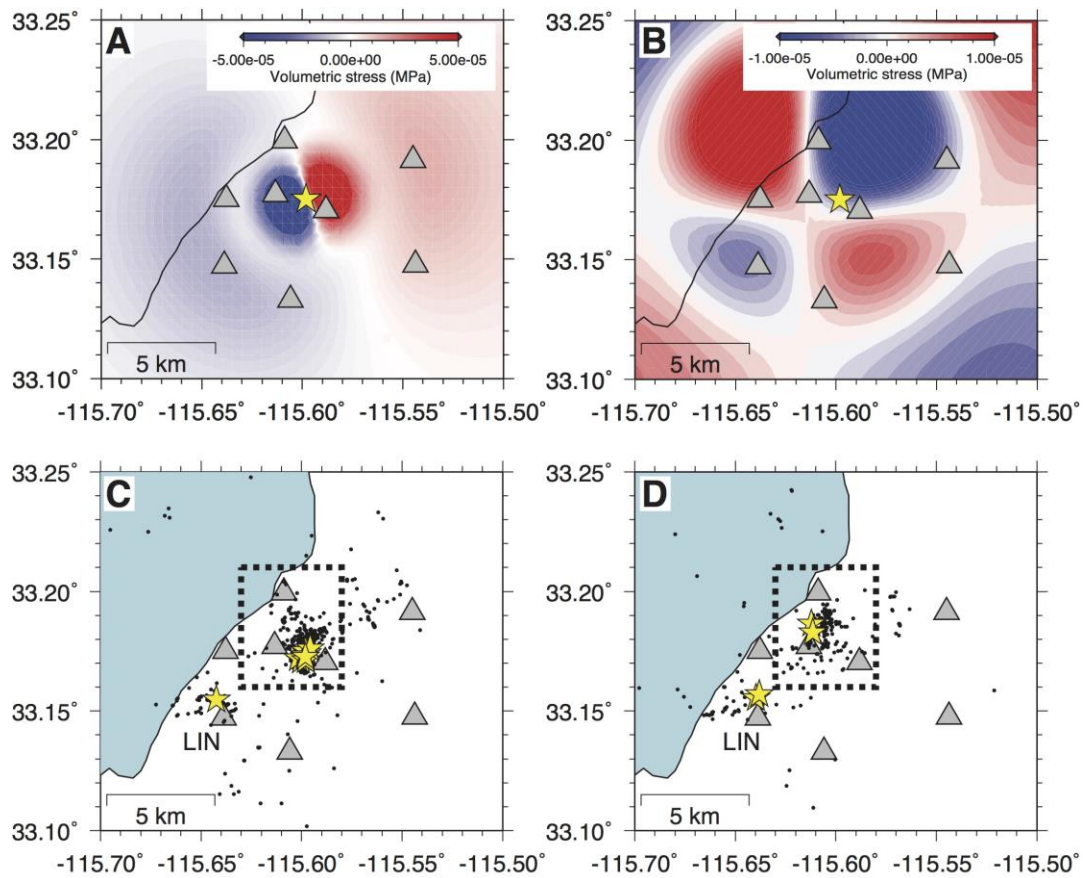


fig. S17. Volumetric static stress change and seismicity map. Volumetric static stress changes at a depth of 1 km imparted by (A) the 18 November 2009 M_w 3.38 and (B) the 28 December 2010 M_w 3.76 earthquakes. Map views of (C) the 2009 earthquake and (D) the 2010 earthquake swarms. Dashed rectangles in (C) and (D) indicates the areas shown in Fig. 3C and 3D, respectively. Black dots are relocated earthquake locations with a waveform cross-correlation analysis (77). Yellow stars show the epicenters of the M 3+ earthquakes. Earthquakes in the first 100 days from the first earthquake of the earthquake swarms were plotted.

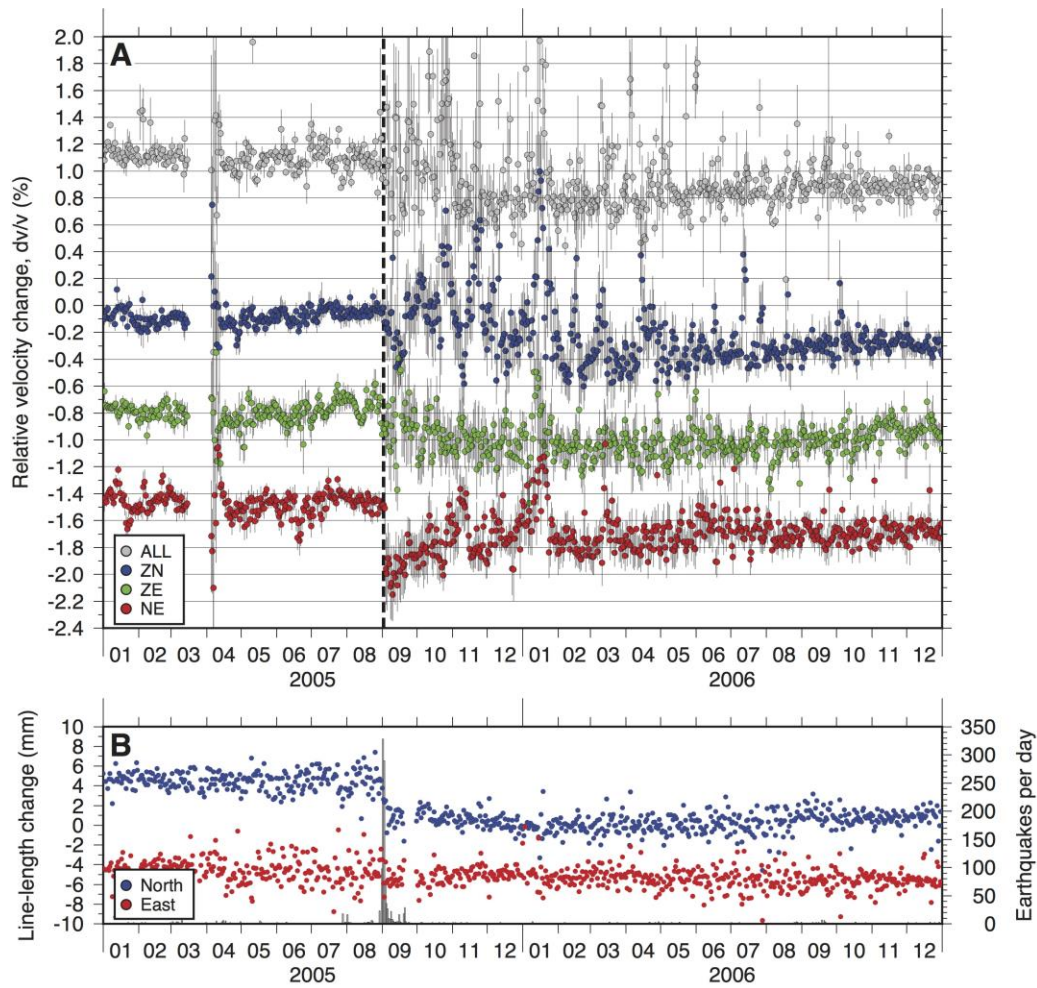


fig. S18. Possible velocity change during the 2005 OB earthquake swarm. (A) Time history of seismic velocity (dv/v) at station RXH in a frequency range of 0.5-2.0 Hz in the time intervals 2005-2006. Black dashed line is the occurrence time of the 2 September 2005 M_w 5.1 earthquake. **(B)** Horizontal Global Positioning System (GPS) line-length change between stations CRRS and GLRS. They are located ~15 km away from the 2005 earthquake. GPS solutions (detrended data) determined by U.S. Geological Survey (<https://earthquake.usgs.gov/monitoring/gps>) were used. The one-sigma error ranges from 2-4 mm for both horizontal components. Also shown are the numbers of earthquakes per

day that occurred within the Salton Sea Geothermal Field (shown in Fig. 1) extracted from a earthquake relocated (77).

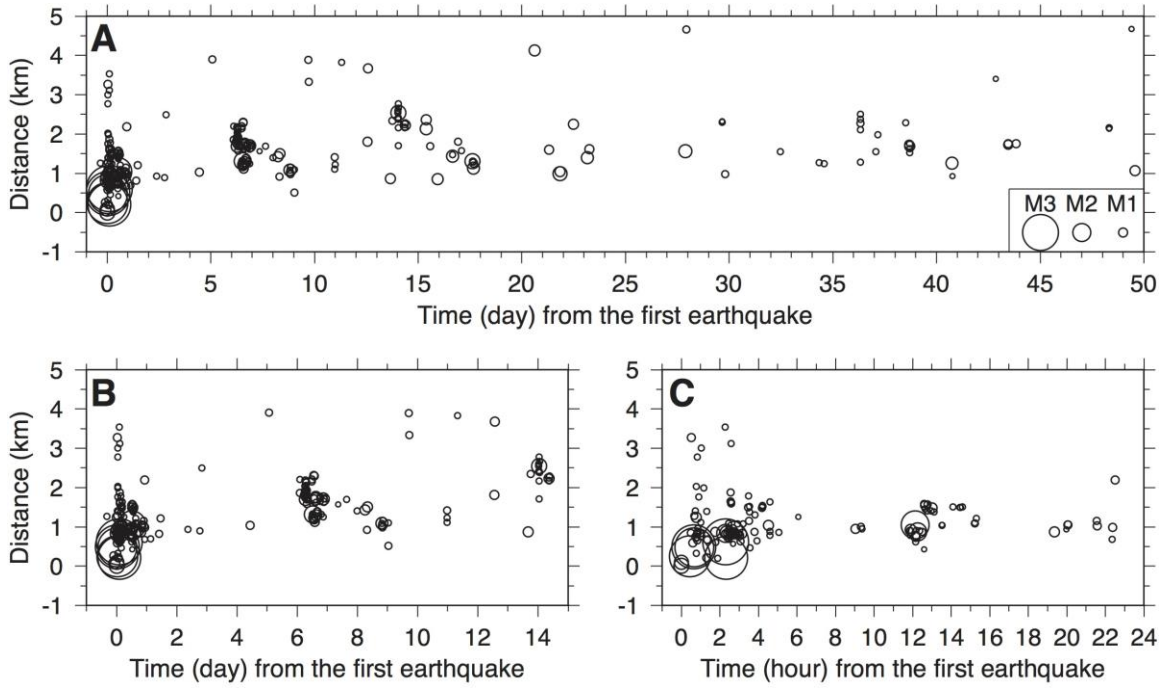


fig. S19. The November 2009 earthquake swarm. (A to C) Distance from the first earthquake in the time intervals (A) -1 through 50 days, (B) -1 through 15 days, and (C) -1 through 24 hours. Circle sizes are proportional to earthquake magnitudes. Relocated earthquake locations with a waveform cross-correlation analysis (77) were used.

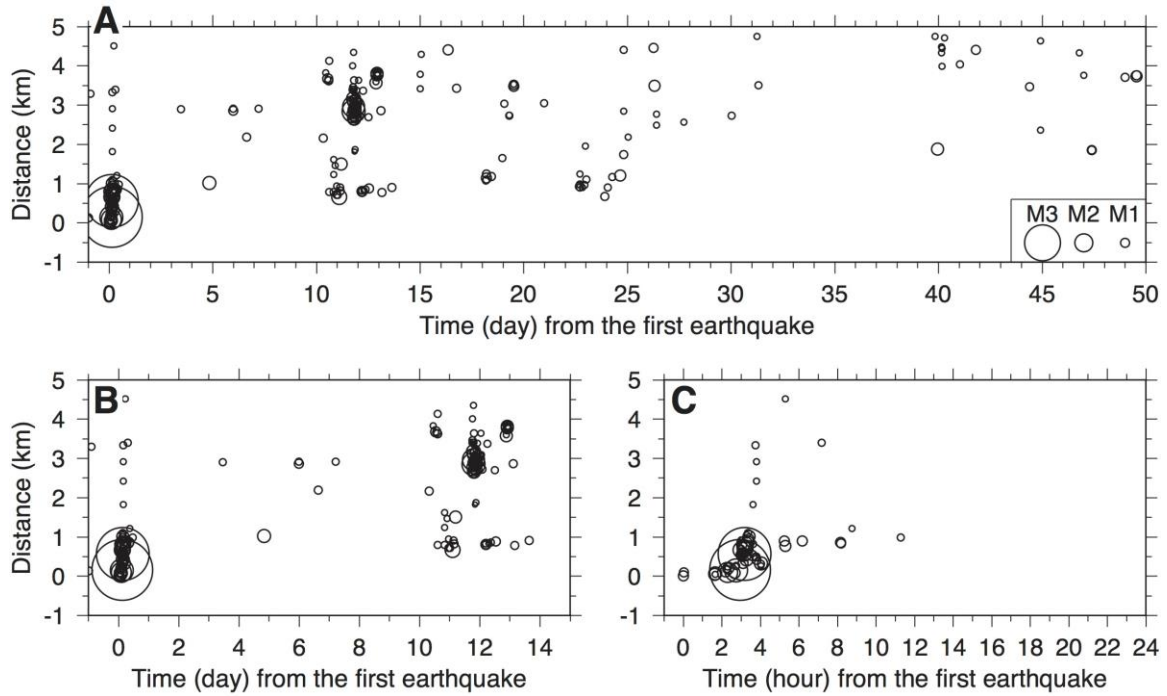


fig. S20. The December 2010 earthquake swarm. (A to C) Distance from the first earthquake in the time intervals (A) -1 through 50 days, (B) -1 through 15 days, and (C) -1 through 24 hours. Circle sizes are proportional to earthquake magnitudes. Relocated earthquake locations with a waveform cross-correlation analysis (77) were used.

table S1. Parameters of the best-fitting curve to observed seismic velocity changes with Eq. 1 and variance reduction (VR).

Station	<i>A</i> (%)	<i>B</i> (%/yr)	<i>C</i> (%)	<i>D</i> (yr)	<i>E</i> (%)	<i>F</i> (%)	<i>J</i> (%)	<i>K</i> (%)	<i>VR</i> (%)
BC3	-0.038	0.011	-0.013	1.026	0.006	0.040	0.008	-0.006	63
BLY	0.060	-0.024	-0.000	0.000	0.016	0.123	0.018	0.028	75
BOM	-0.066	0.019	-0.020	1.323	-0.001	-0.005	0.008	0.007	79
BOR	-0.029	0.017	-0.080	1.753	-0.012	-0.006	-0.003	0.003	82
BTC	0.032	-0.010	-0.001	2.034	-0.023	-0.022	-0.010	-0.007	49
DRE	0.043	0.031	-0.224	75.000	-0.006	-0.010	-0.007	-0.001	87
GLA	0.151	-0.046	-0.050	5.579	-0.016	0.065	-0.000	0.007	72
RXH	-0.152	0.060	-0.143	0.421	-0.045	0.010	0.010	0.002	96
SAL	-0.004	0.003	-0.000	0.000	-0.016	-0.022	0.005	-0.003	43
SWS	-0.004	0.018	-0.142	2.985	-0.017	-0.014	0.001	-0.002	87
WES	0.144	0.011	-0.289	45.086	-0.014	-0.009	-0.007	-0.002	91
MONP2	-0.011	0.013	-0.055	11.697	-0.008	-0.012	0.001	-0.000	58
EN*	-0.096	0.040	-0.251	0.338	-0.012	-0.005	0.001	-0.003	88
			<i>C</i> ₂ (%)	<i>D</i> ₂ (yr)					
EN*			-0.101	0.446					

*EN represents the two-station cross-correlation analysis of the CalEnergy stations (EN network) shown in Fig 1.

table S2. PGV from the SCEDC and stress sensitivity estimate for the 4 April 2010

***M_w* 7.2 El Mayor–Cucapah earthquake.**

Station	PGV (cm/s)	Velocity change** (%)	Stress sensitivity (MPa ⁻¹)
BC3	1.77*	-0.013	-0.000119
BLY	1.61	-0.000	-0.000000
BOM	9.26*	-0.020	-0.000355
BOR	5.84*	-0.080	-0.002249
BTC	9.38*	-0.001	-0.000018
DRE	29.66	-0.224	-0.001240
GLA	3.42	-0.050	-0.002403
RXH	7.47	-0.143	-0.003138
SAL	1.23	-0.000	-0.000000
SWS	10.40*	-0.142	-0.002241
WES	55.54*	-0.289	-0.000854
MONP2	8.03	-0.055	-0.001129

*PGVs manually obtained by measuring the absolute peak amplitude on strong-motion seismic data

**Values of velocity changes are the same as the parameter C listed in table S1.